Correlations in nondegenerate parametric oscillation: Squeezing in the presence of phase diffusion

M. D. Reid
Department of Physics, University of Waikato, Hamilton, New Zealand

P. D. Drummond
Department of Physics, University of Queensland, Saint Lucia, Brisbane, Australia
(Received 13 March 1989)

We present a quantum theory of the nondegenerate parametric oscillator above threshold. The effect of signal and idler phase diffusion on the various types of external squeezing spectral measurements is discussed.

I. INTRODUCTION

There has been recent interest and success in generating squeezed states of light.[1] Possible applications include ultrasensitive interferometry[2,3] and spectroscopy.[4] Some recent efforts have focused on trying to generate squeezed light with a nonzero coherent amplitude.[4,5] Heidmann *et al.*[4] have recently achieved a reduction of intensity difference fluctuations in the nondegenerate parametric oscillator. This comes about because the signal and idler intensity fluctuations are correlated. Similar correlations occurring at much lower intensities in nondegenerate parametric amplification have also been demonstrated.[6,7]

The experimental interest in the quantum behavior of the nondegenerate parametric oscillator has been complemented by several recent theoretical works.[8–12] Early quantum theories were presented by Graham and Haken.[13] McNeil and Gardiner[14] gave the first squeezing calculation for the intracavity field. From these analyses it is apparent that the nondegenerate parametric oscillator displays a mode of oscillation above threshold which is very different from the degenerate case. In the degenerate case, the oscillation above threshold displays bistability. There are two possible metastable phases that are available for oscillation. The theoretical treatments of this problem usually involve a linearization around one of these metastable phases.[15,16] After linearizing, it is found that the oscillator produces squeezed radiation.[16] However, this neglects the possible quantum switching on long time scales that can occur between the phases. The radiation is different to that produced below the threshold, since the above-threshold radiation has a coherent part whose coherence time is very long compared to the decay time of the interferometer.

In the nondegenerate case, there is a continuum of above-threshold phases for the signal and idler modes.[13,17] The parametric oscillator undergoes a steady phase diffusion amongst its possible output phases. Well above threshold the rate of phase diffusion is reduced.[13] The recent analyses of Reynaud *et al.*[8] and Björk and Yamamoto[9] essentially assume this limit and linearize fluctuations, thus assuming that the phase is stable. Such analyses predict squeezing in certain combinations of the output signal and idler.

The presence of the phase diffusion in the signal and idler mode will, produce a coherent part in the output radiation with a finite coherence time greater than the decay time of the interferometer. Thus we expect large phase fluctuations at low frequencies. Previous calculations of noise spectra have not analyzed this effect. It is our aim to present an analysis of the nondegenerate parametric oscillator which includes the effect of the phase diffusion on the various types of external squeezing spectral measurements. We find that squeezing does occur in the above-threshold output radiation. Phase diffusion tends to destroy this nonclassical effect at sufficiently low frequencies.

II. DERIVATION OF STOCHASTIC EQUATIONS

A standard procedure is used to analyze the optical nondegenerate parametric oscillator. The parametric oscillation occurs via a nonlinear medium placed inside a suitably tuned optical cavity. Three near resonant intracavity modes are considered, of frequencies ω_1, ω_2, and ω_3, where $\omega_1+\omega_2=\omega_3$. This implies that $\omega_{1,2}=\omega_0\pm\epsilon$, where $\omega_0=\omega_3/2$. The field at frequency ω_3 is pumped by a resonant external driving field. The model Hamiltonian for the system is taken to be, in the rotating-wave approximation,

$$H=H_{\rm rev}+H_{\rm irrev}\ , \tag{2.1}$$

where

$$\begin{aligned}H_{\rm rev}&=h\omega_1\hat{a}_1^{\dagger}\hat{a}_1+h\omega_2\hat{a}_2^{\dagger}\hat{a}_2+h\omega_3\hat{a}_3^{\dagger}\hat{a}_3\\&\quad+i\hbar g(\hat{a}_1^{\dagger}\hat{a}_2^{\dagger}\hat{a}_3-\hat{a}_1\hat{a}_2\hat{a}_3^{\dagger})\\&\quad+i\hbar[E\hat{a}_3^{\dagger}\exp(-i\omega_3 t)-E^*\hat{a}_3\exp(i\omega_3 t)]\ ,\\H_{\rm irrev}&=\hat{a}_1\hat{\Gamma}_1^{\dagger}+\hat{a}_1^{\dagger}\hat{\Gamma}_1+\hat{a}_2\hat{\Gamma}_2^{\dagger}+\hat{a}_2^{\dagger}\hat{\Gamma}_2+\hat{a}_3\hat{\Gamma}_3^{\dagger}+\hat{a}_3^{\dagger}\hat{\Gamma}_3\ .\end{aligned}$$

Here, ω_1, ω_2, and ω_3 are the signal, idler, and pump frequencies, respectively. The term g describes the non-

linear coupling due to the medium and E is the input driving amplitude. The $\hat{a}_i, \hat{a}_i^\dagger$ are boson annihilation and creation operators for the cavity modes at frequency ω_i. The decay of the cavity modes to the external modes of the field outside the cavity are described by the reservoirs $\hat{\Gamma}_1$, $\hat{\Gamma}_2$, and $\hat{\Gamma}_3$. This decay will give rise to cavity damping rates κ_1, κ_2, and κ_3 for the cavity modes $\hat{a}_1$, $\hat{a}_2$, and $\hat{a}_3$, respectively. For simplicity we consider all detunings to be zero. We also assume that the modes decay into distinct uncorrelated reservoirs, and hence that the cavity linewidths are small compared to the cavity spacing and the resonant frequencies. However, the treatment holds for the case of $\omega_1=\omega_2$ provided these modes have orthogonal polarizations. For nonorthogonal polarizations, we require that the signal-idler detuning ϵ is much larger than either of the cavity linewidths.

This model Hamiltonian has been studied by previous authors.[13,14] We follow the procedure used previously[14,18] to obtain an equation of motion for the density operator $\hat{\rho}$ as a master equation. This is achieved by transforming to an interaction picture in which all operators rotate in the frame related to that of the driving field,

$$\hat{a}_j(t)=\hat{a}_j e^{-i\omega_j t}, \quad \hat{a}_j^\dagger(t)=\hat{a}_j^\dagger e^{i\omega_j t} . \tag{2.2}$$

Standard techniques are then applied to convert the master equation into a c-number Fokker-Planck equation.

The density operator $\hat{\rho}$ is expanded in a positive P representation[19] so that

$$\hat{\rho}=\int \frac{|\boldsymbol{\alpha}\rangle\langle\boldsymbol{\alpha}^\dagger|}{\langle\boldsymbol{\alpha}^\dagger|\boldsymbol{\alpha}\rangle} P(\boldsymbol{\alpha},\boldsymbol{\alpha}^\dagger) d^6\boldsymbol{\alpha} d^6\boldsymbol{\alpha}^\dagger , \tag{2.3}$$

where

$$\boldsymbol{\alpha}\equiv(\alpha_1,\alpha_2,\alpha_3), \quad \boldsymbol{\alpha}^\dagger\equiv(\alpha_1^\dagger,\alpha_2^\dagger,\alpha_3^\dagger) .$$

There is thus a correspondence between the c numbers α_i and $\alpha_i^\dagger$, and the operators $\hat{a}_i$ and $\hat{a}_i^\dagger$. In this representation α_i and $\alpha_i^\dagger$ are independent complex variables. The Fokker-Planck equation derived can be transformed into the following stochastic differential equations:[11,18]

$$\begin{aligned}
\dot{\alpha}_1 &= -\kappa\alpha_1+g\alpha_3\alpha_2^\dagger+(g\alpha_3)^{1/2}\zeta_1(t) , \\
\dot{\alpha}_2 &= -\kappa\alpha_2+g\alpha_3\alpha_1^\dagger+(g\alpha_3)^{1/2}\zeta_2(t) , \\
\dot{\alpha}_3 &= E-\kappa_3\alpha_3-g\alpha_1\alpha_2 , \\
\dot{\alpha}_1^\dagger &= -\kappa\alpha_1^\dagger+g\alpha_3^\dagger\alpha_2+(g\alpha_3^\dagger)^{1/2}\zeta_1^\dagger(t) , \\
\dot{\alpha}_2^\dagger &= -\kappa\alpha_2^\dagger+g\alpha_3^\dagger\alpha_1+(g\alpha_3^\dagger)^{1/2}\zeta_2^\dagger(t) , \\
\dot{\alpha}_3^\dagger &= E^*-\kappa_3\alpha_3^\dagger-g\alpha_1^\dagger\alpha_2^\dagger ,
\end{aligned} \tag{2.4a}$$

where $\zeta_i(t)$ and $\zeta_i^\dagger(t)$ are independent real noise sources with nonzero correlations,

$$\begin{aligned}
\langle\zeta_1(t)\zeta_2(t')\rangle &= \delta(t-t') , \\
\langle\zeta_1^\dagger(t)\zeta_2^\dagger(t')\rangle &= \delta(t-t') .
\end{aligned} \tag{2.4b}$$

We have taken for simplicity $\kappa_1=\kappa_2=\kappa$. These equations have been derived and studied, in part, before.[18] We note that an alternative stochastic method of Graham used the Wigner representation.[13]

The equations of motion for the classical (slowly varying) amplitudes are recovered from Eq. (2.4) by simply dropping the noise functions $\zeta_i(t)$. The steady-state semiclassical solutions are readily derived by solving with all time derivatives put equal to zero and with $\alpha_i^\dagger=\alpha_1^*$. The steady-state solution α_1^0 is therefore[14]

$$\alpha_1^0=\alpha_2^0=0, \quad \alpha_3^0=E/\kappa_3 \quad \text{for } |E|<\frac{\kappa_3\kappa}{g} \tag{2.5a}$$

or

$$|\alpha_3^0|^2=\frac{\kappa^2}{g^2}, \quad |\alpha_1^0|^2=|\alpha_2^0|^2=\frac{|E|}{g}-\frac{\kappa_3\kappa}{g^2} \quad \text{for } |E|>\frac{\kappa_3\kappa}{g} . \tag{2.5b}$$

Thus $|\alpha_i^0|^2$ is the steady-state semiclassical intensity (in units of photon number). The stability of these solutions with respect to small fluctuations is checked by deriving the linearized equations of motion for the fluctuations $\delta\alpha_i=\alpha_i-\alpha_i^0$. The solutions are stable provided the eigenvalues of the appropriate drift matrix of the linearized equations are positive. The solution (2.5a) is called the below-threshold solution since it is stable for, and only for, a driving field amplitude E satisfying $|E|<E_T$, where $E_T=\kappa_3\kappa/g$ denotes the threshold driving field intensity. The detailed properties of this situation will be treated in another paper.[18]

In this paper we consider only the situation of large threshold photon numbers (corresponding to large $\kappa_3\kappa/g^2$). In this case, which corresponds to all current optical experiments, the effect of quantum noise is to cause small perturbations about the stable steady-state semiclassical solutions (2.5), where $\alpha_i^{\dagger 0}=\alpha_i^{0*}$.[20] We therefore study the quantum properties by linearizing about the classical deterministic solutions only, ignoring the nonclassical deterministic solutions with $\alpha_i^{\dagger 0}\neq\alpha_i^{0*}$.

III. ABOVE-THRESHOLD EQUATIONS AND SOLUTIONS

We now wish to analyze the stochastic equations (2.4) above threshold. An analysis of the equations, linearized about the solutions (2.5b), reveals the presence of a zero eigenvalue. The system is not stable and cannot be analyzed correctly by the assumption of small fluctuations and methods of linearization. This is physically due to phase diffusion in the signal and idler modes. A similar situation exists in the laser above threshold.[21] We follow the standard approach used for the laser problem and transform to phase and amplitude variables, noting that the stochastic equations (2.4) are equivalent in either Ito or Stratonovic formulations of the stochastic calculus. From now on, we will use the Stratonovic form of the stochastic calculus, which permits variable changes without any extra variable-change terms. In the intensity and amplitude variables, the stochastic equations become

$$
\begin{aligned}
\dot{I}_1 &= -2\kappa I_1 + 2g(I_1 I_2 I_3)^{1/2}\cos\psi + F_1(t) , \\
\dot{\phi}_1 &= -g(I_3 I_2 / I_1)^{1/2}\sin\psi + f_1(t) , \\
\dot{I}_2 &= -2\kappa I_2 + 2g(I_1 I_2 I_3)^{1/2}\cos\psi + F_2(t) , \\
\dot{\phi}_2 &= -g(I_3 I_1 / I_2)^{1/2}\sin\psi + f_2(t) , \\
\dot{I}_3 &= 2|E| I_3^{1/2}\cos(\phi_3 - \phi_0) - 2\kappa_3 I_3 \\
&\quad - 2g(I_1 I_2 I_3)^{1/2}\cos\psi , \\
\dot{\phi}_3 &= -|E| I_3^{-1/2}\sin(\phi_3 - \phi_0) - g(I_1 I_2 / I_3)^{1/2}\sin\psi .
\end{aligned}
\tag{3.1}
$$

Here I_j, ϕ_j have the obvious definitions in terms of the stochastic variables $\alpha_j, \alpha_j^\dagger$, while ψ is an auxiliary phase,

$$
\begin{aligned}
I_j &= \alpha_j \alpha_j^\dagger , \\
\phi_j &= \ln(\alpha_j^\dagger / \alpha_j)/2i , \quad j = 1,2,3 \\
\psi &= \phi_1 + \phi_2 - \phi_3 .
\end{aligned}
\tag{3.2}
$$

We have written the external driving field as $E = |E| e^{-i\phi_0}$. The stochastic forces $\mathbf{F}(t), \mathbf{f}(t)$ are defined as

$$
\begin{aligned}
F_j(t) &= (g\alpha_3)^{1/2}\alpha_j \xi_j^\dagger(t) + (g\alpha_3)^{1/2}\alpha_j^\dagger \xi_j(t) , \\
f_j(t) &= (g\alpha_3^\dagger)^{1/2}\xi_j^\dagger(t)/(2i\alpha_j^\dagger) - (g\alpha_3)^{1/2}\xi_j(t)/(2i\alpha_j) .
\end{aligned}
\tag{3.3}
$$

It should be noted again that in the positive P representation used here, the α_j and $\alpha_j^\dagger$ are independent complex amplitudes. This implies that I_j, ϕ_j are complex stochastic variables, and it is this complex character that directly results in nonclassical behavior in the output fields. This, in fact, causes no additional algebraic problems, since the observables are all analytic functions of I_j, ϕ_j.

The above-threshold steady-state semiclassical solutions in terms of the intensity and phase variables are

$$
\begin{aligned}
I_3^0 &= |E|^2/\kappa_3^2 , \quad I_1^0 = I_2^0 = \frac{|E|}{g} - \frac{\kappa_3 \kappa}{g^2} , \\
\psi^0 &= 0 , \quad \phi_3^0 = \phi_0 .
\end{aligned}
\tag{3.4}
$$

We see the pump phase ϕ_3^0 and the signal-idler sum phase $\phi_1^0 + \phi_2^0$ are locked to ϕ_0, the phase of the external driving field. However, unlike the below-threshold solution, there is no unique solution for the signal and idler amplitudes themselves. The individual phases ϕ_1^0 and ϕ_2^0 are arbitrary. For this reason a linearized eigenvalue analysis around any chosen phase ϕ will always generate a zero eigenvalue. This property of the nondegenerate parametric oscillator has already been noted and discussed by Graham and Haken[13] and Brunner and Paul.[17]

To correctly analyze Eq. (3.1), it is helpful to factorize the equations into a part which is stable and a part that undergoes phase diffusion. Following this, the stable set can be linearized, while the equations associated with the zero eigenvalue must be treated exactly without linearization. A similar procedure was used by Graham and Haken,[13] who analyzed the nondegenerate parametric oscillator with quantum operator equations.

Accordingly we write Eq. (3.1) in terms of new variables $\phi_\pm = \phi_1 \pm \phi_2$:

$$
\begin{aligned}
\dot{I}_1 &= -2\kappa I_1 + 2g(I_3 I_2 I_1)^{1/2}\cos\psi + F_1(t) , && \text{(3.5a)} \\
\dot{I}_2 &= -2\kappa I_2 + 2g(I_3 I_2 I_1)^{1/2}\cos\psi + F_2(t) , && \text{(3.5b)} \\
\dot{\phi}_+ &= [-g(I_3 I_2 / I_1)^{1/2} - g(I_3 I_1 / I_2)^{1/2}]\sin\psi \\
&\quad + f_1(t) + f_2(t) , && \text{(3.5c)} \\
\dot{I}_3 &= -2\kappa_3 I_3 + 2|E| I_3^{1/2}\cos\phi_3 - 2g(I_3 I_2 I_1)^{1/2}\cos\psi , && \text{(3.5d)} \\
\dot{\phi}_3 &= -|E| I_3^{-1/2}\sin\phi_3 - g(I_1 I_2 / I_3)^{1/2}\sin\psi , && \text{(3.5e)} \\
\dot{\phi}_- &= [-g(I_3 I_2 / I_1)^{1/2} + g(I_3 I_1 / I_2)^{1/2}]\sin\psi \\
&\quad + f_1(t) - f_2(t) . && \text{(3.5f)}
\end{aligned}
$$

We have taken for notational convenience $\phi_0 = 0$.

Equations (3.5a)–(3.5e) describe the behavior of the variables I_j, ψ, and ϕ_3, which have a unique steady-state solution. It is possible to linearize this subset for the fluctuations about the steady-state solutions, since we will show the linearized equations to be stable. Thus we define

$$
\begin{aligned}
\Delta I_j &= I_j - I_j^0 , \\
\Delta\phi_+ &= \phi_1 + \phi_2 - \phi_0 , \\
\Delta\phi_3 &= \phi_3 - \phi_0 ,
\end{aligned}
\tag{3.6}
$$

and linearize Eq. (3.5) with respect to I_j, ϕ_+, and ϕ_3. The linearization procedure is an excellent approximation provided the size of the quantum noise is not too large, i.e., provided we have a large threshold photon number: $\kappa_3 \kappa / g^2 \gg 1$. This is the situation of all current optical experiments. With the partial linearization (3.6), Eqs. (3.5) may then be rewritten as follows:

$$
\begin{aligned}
\Delta\dot{I}_+ &= (2g^2 I^0/\kappa)\Delta I_3 + F_+^0(t) , \\
\Delta\dot{I}_3 &= -\kappa_3 \Delta I_3 - \kappa \Delta I_+ , \\
\Delta\dot{I}_- &= -2\kappa \Delta I_- + F_-^0(t) , \\
\Delta\dot{\phi}_+ &= -2\kappa\Delta\phi_+ + 2\kappa\Delta\phi_3 + f_+^0(t) , \\
\Delta\dot{\phi}_3 &= -\kappa_3\Delta\phi_3 - (g^2 I^0/\kappa)\Delta\phi_+ , \\
\dot{\phi}_- &= f_-^0(t) ,
\end{aligned}
\tag{3.7}
$$

where

$$
\Delta I_\pm = \Delta I_1 \pm \Delta I_2
$$

and the non-zero noise correlations are

$$
\begin{aligned}
\langle F_+^0(t) F_+^0(t') \rangle &= -\langle F_-^0(t) F_-^0(t') \rangle = 4\kappa I^0 \delta(t - t') , \\
\langle f_-^0(t) f_-^0(t') \rangle &= -\langle f_+^0(t) f_+^0(t') \rangle = (\kappa / I^0)\delta(t - t') .
\end{aligned}
$$

We have defined $I^0 = I_1^0 = I_2^0$. The noise correlations are functions of ψ and I_j which are stable about their steady-state values. Hence in this linearized theory ψ and I_j may be replaced by ψ^0 and I_j^0 in the noise correlations. The signal-idler difference phase ϕ_- is not describable as a small fluctuation about a stable steady-state value. The ΔI_j, $\Delta\phi_+$, and $\Delta\phi_3$ are damped quantities and thus have

stable points of $\Delta I_j=\Delta\phi_+=\Delta\phi_3=0$, while ϕ_- is not damped and can undergo a continuous phase diffusion.

For the case we have considered here of zero detunings and equal signal and idler decay rates, Eqs. (3.7) decouple into four subsystems. These subsystems are of the linear form $\dot{\mathbf{x}}=-\underline{A}\mathbf{x}+\mathbf{F}(t)$, where $\underline{A}$ is a matrix, and are hence readily solved. The eigenvalues λ of the matrix $\underline{A}$ can be readily calculated in all cases.

First we examine the equations for the intensity variables above threshold. The intensity difference ΔI_- decouples from ΔI_3 and ΔI_+ completely and therefore has the immediate solution

$$\Delta I_-(t)=\Delta I_-(t_0)e^{-2\kappa(t-t_0)}+\int_{t_0}^{t}e^{2\kappa(t'-t)}F_-^0(t')dt' , \tag{3.8}$$

where t_0 is the initial time. The fluctuation ΔI_- in the intensity difference between the signal and idler is stable, decaying to the steady-state value of zero with relaxation time $(2\kappa)^{-1}$.

The pump intensity ΔI_3 and signal-idler sum intensity ΔI_+ fluctuations are coupled. The eigenvalues of this subsystem are found to be

$$\lambda_{1,2}=[\kappa_3\pm(\kappa_3^2-8g^2I^0)^{1/2}]/2 \tag{3.9}$$

and the solutions in the long-time limit are

$$\begin{aligned}\Delta I_+(t)&=\tfrac{1}{2}A_1\int_{-\infty}^{t}e^{\lambda_1(t'-t)}F_+^0(t')dt'\\&\quad+\tfrac{1}{2}A_2\int_{-\infty}^{t}e^{\lambda_2(t'-t)}F_+^0(t')dt' ,\\\Delta I_3(t)&=\frac{\kappa}{(\kappa_3^2-8g^2I^0)^{1/2}}\\&\quad\times\left[\int_{-\infty}^{t}e^{\lambda_1(t'-t)}F_+^0(t')dt'\right.\\&\quad\left.-\int_{-\infty}^{t}e^{\lambda_2(t'-t)}F_+^0(t')dt'\right] ,\end{aligned} \tag{3.10}$$

where

$$A_{1,2}=1\mp\frac{\kappa_3}{(\kappa_3^2-8g^2I^0)^{1/2}} .$$

We note that the eigenvalues (3.9) have positive real parts and hence the ΔI_3, ΔI_+ subsystem is stable.

Equations (3.7) for the phase variables above threshold also decouple into two subsystems. The decoupled difference phase ϕ_- equation describes the larger undamped fluctuations due to phase diffusion. The solution for ϕ_- and hence its correlation function are immediate,

$$\phi_-(t)=\phi_-(t_0)+\int_{t_0}^{t}f_-^0(t')dt' . \tag{3.11}$$

The phase diffusion implies that

$$\langle[\phi_-(t+\tau)-\phi_-(t)]^2\rangle=\kappa|\tau|/I^0 . \tag{3.12}$$

This was calculated by Graham and Haken,[13] who used quantum operator equations.

The $\Delta\phi_3,\Delta\phi_+$ subsystem describes damped fluctuations in the pump and signal-idler sum phase. The eigenvalues of the $\Delta\phi_3$, $\Delta\phi_+$ subsystem are, using Eqs. (3.4) and (3.7),

$$\bar{\lambda}_{1,2}=(\kappa+\kappa_3/2)\pm[(\kappa+\kappa_3/2)^2-2g|E|]^{1/2} . \tag{3.13}$$

These have positive real parts, ensuring stability. The long-time solutions are found to be

$$\begin{aligned}\Delta\phi_+(t)&=\tfrac{1}{2}\bar{A}_1\int_{-\infty}^{t}e^{\bar{\lambda}_1(t'-t)}f_+^0(t')dt'\\&\quad+\tfrac{1}{2}\bar{A}_2\int_{-\infty}^{t}e^{\bar{\lambda}_2(t'-t)}f_+^0(t')dt'\end{aligned}$$

and

$$\begin{aligned}\Delta\phi_3(t)&=\frac{g^2I^0/\kappa}{[(2\kappa+\kappa_3)^2-8g|E|]^{1/2}}\\&\quad\times\left[\int_{-\infty}^{t}e^{\bar{\lambda}_1(t'-t)}f_+^0(t')dt'\right.\\&\quad\left.-\int_{-\infty}^{t}e^{\bar{\lambda}_2(t'-t)}f_+^0(t')dt'\right]\end{aligned} \tag{3.14}$$

where

$$\bar{A}_{1,2}=1\pm\frac{(2\kappa-\kappa_3)}{[(2\kappa+\kappa_3)^2-8g|E|]^{1/2}} .$$

IV. CALCULATION OF TWO-TIME CORRELATION FUNCTIONS AND SPECTRA

We next wish to calculate the nonzero two-time correlation functions of the type $\langle\hat{\Phi}_j^\dagger(t)\hat{\Phi}_j(t+\tau)\rangle$ and $\langle\hat{\Phi}_i(t)\hat{\Phi}_j(t+\tau)\rangle$ above threshold. Here we introduce the photon-amplitude operators $\hat{\Phi}_j$ for the field external to the interferometer. We follow the notation of Mandel and Cook,[22] except that we use $\langle\hat{\Phi}^\dagger\hat{\Phi}\rangle$ to indicate the integrated photon emission rate, not the photon density.[18] In the case that the only signal and idler cavity losses are through single output couplers with perfect mode matching for each mode, these operator moments correspond to stochastic two-time correlation functions[23] so that

$$\begin{aligned}&(2\kappa)^{-1}\langle\hat{\Phi}_1^\dagger(t)\hat{\Phi}_1(t+\tau)\rangle\\&\quad=\langle\alpha_1^\dagger(t)\alpha_1(t+\tau)\rangle\\&\quad=\langle\sqrt{I_1(t)}e^{i\phi_1(t)}\sqrt{I_1(t+\tau)}e^{-i\phi_1(t+\tau)}\rangle ,\\&(2\kappa)^{-1}\langle\hat{\Phi}_1(t)\hat{\Phi}_2(t+\tau)\rangle=\langle\alpha_1(t)\alpha_2(t+\tau)\rangle .\end{aligned} \tag{4.1}$$

For small signal-idler sum phase and intensity fluctuations one can linearize so that

$$\begin{aligned}\sqrt{I_{1,2}(t)}&=\sqrt{I^0}[1+\Delta I_{1,2}(t)/(2I^0)]\\&=(I^0)^{1/2}[1+(\Delta I_+\pm\Delta I_-)/4I^0] ,\\\phi_{1,2}(t)&=\tfrac{1}{2}[\Delta\phi_+(t)\pm\phi_-(t)] .\end{aligned} \tag{4.2}$$

Thus in the linear approximation

$$\begin{aligned}\langle\alpha_1^\dagger(t)\alpha_1(t+\tau)\rangle&=I^0\langle[1+\Delta I_1(t)/(2I^0)][1+\Delta I_1(t+\tau)/(2I^0)][1+i\Delta\phi_+(t)/2][1-i\Delta\phi_+(t+\tau)/2]\\&\quad\times\exp\{i[\phi_-(t)-\phi_-(t+\tau)]/2\}\rangle .\end{aligned} \tag{4.3}$$

We have included, to first order, only terms such as $\langle \Delta\phi_+(t)\Delta\phi_+(t+\tau)\rangle$ which involve two times, since these are the terms giving rise to the broadband incoherent part of the spectrum. There are other terms to first order which contribute corrections to the coherent part of the spectrum. These only make small modifications to the value I^0 in the final result and are ignored here. In this particular problem, $\Delta I_1(t)$, $\Delta\phi_+(t)$, and $\phi_-(t)$ are uncorrelated in the linear approximation. Hence Eq. (4.3) can be reduced to the simpler form

$$\begin{aligned}\langle \alpha_1^\dagger(t)\alpha_1(t+\tau)\rangle/=I^0[1+\langle \Delta I_1(t)\Delta I_1(t+\tau)\rangle/(2I^0)^2 \\ +\langle \Delta\phi_+(t)\Delta\phi_+(t+\tau)\rangle/4] \\ \times\langle \exp\{i[\phi_-(t)-\phi_-(t+\tau)]/2\}\rangle .\end{aligned} \tag{4.4}$$

The long-time or steady-state intensity correlations are readily calculated from our solutions (3.8)–(3.10):

$$\begin{aligned}&\langle \Delta I_-(t)\Delta I_-(t+\tau)\rangle = -I^0 e^{-2\kappa|\tau|} , \\ &\langle \Delta I_+(t)\Delta I_+(t+\tau)\rangle \\ &\quad =\kappa I^0\left[\frac{A_1^2}{2\lambda_1}+\frac{A_1A_2}{\lambda_1+\lambda_2}\right]e^{-\lambda_1|\tau|} \\ &\quad +\kappa I^0\left[\frac{A_2^2}{2\lambda_2}+\frac{A_1A_2}{\lambda_1+\lambda_2}\right]e^{-\lambda_2|\tau|} .\end{aligned} \tag{4.5}$$

Similarly, the sum-phase correlation is, for (3.14),

$$\begin{aligned}&\langle \Delta\phi_+(t)\Delta\phi_+(t+\tau)\rangle \\ &\quad =\frac{-\kappa}{4I^0}\left[\frac{\bar{A}_1^2}{2\bar{\lambda}_1}+\frac{\bar{A}_1\bar{A}_2}{\bar{\lambda}_1+\bar{\lambda}_2}\right]e^{-\bar{\lambda}_1|\tau|} \\ &\quad -\frac{\kappa}{4I^0}\left[\frac{\bar{A}_2^2}{2\bar{\lambda}_2}+\frac{\bar{A}_1\bar{A}_2}{\bar{\lambda}_1+\bar{\lambda}_2}\right]e^{-\bar{\lambda}_2|\tau|} .\end{aligned} \tag{4.6}$$

We point out that the correlations $\langle \Delta I_-(t)\Delta I_-(t+\tau)\rangle$ and $\langle \Delta\phi_+(t)\Delta\phi_+(t+\tau)\rangle$ of the signal and idler intensity difference and phase-sum variables, respectively, are both negative in the P representation. This indicates a reduction of fluctuations below the shot-noise level. The intensity-sum correlation $\langle \Delta I_+(t)\Delta I_+(t+\tau)\rangle$, in contrast, is positive. A reduction in the signal and idler intensity difference fluctuations was predicted by Reynaud *et al.*[8] and has been experimentally detected by Heidmann *et al.*[4]

Next, it is necessary to calculate the correlation of the signal-idler phase difference $\phi_-(t)$. This diffuses so that one cannot assume small fluctuations. A complex Gaussian variable ξ with zero mean satisfies[21]

$$\langle e^{\xi}\rangle = e^{\langle \xi^2\rangle/2} . \tag{4.7}$$

The variance $\langle [\phi_-(t)-\phi_-(t+\tau)]^2\rangle$ has been calculated from (3.12), and thus

$$\langle \exp\{i[\phi_-(t)-\phi_-(t+\tau)]/2\}\rangle = e^{-\kappa|\tau|/8I^0} . \tag{4.8}$$

The steady-state two-time correlation (4.4) is therefore

$$\begin{aligned}\langle \alpha_1^\dagger(t)\alpha_1(t+\tau)\rangle = I^0 e^{-\kappa|\tau|/(8I^0)}\{1+\langle \Delta\phi_+(t)\Delta\phi_+(t+\tau)\rangle/4 \\ +[\langle \Delta I_-(t)\Delta I_-(t+\tau)\rangle+\langle \Delta I_+(t)\Delta I_+(t+\tau)\rangle]/(4I^0)^2\} .\end{aligned} \tag{4.9}$$

The first or leading term ($I^0 e^{-\kappa|\tau|/8I^0}$) in (4.9) describes a decorrelation over a time $\tau_c = 8I^0/\kappa$ due to phase diffusion. In our analysis here we have linearized the I_j, ϕ_3, and ϕ_+ variables, which is valid for large I^0. This approximation will break down for smaller I^0 near threshold where fluctuations become large. As I^0 increases above threshold the decorrelation time $8I^0/\kappa$ becomes very large. The phase diffusion in this leading term will show up in the intensity spectrum as a very large but narrow Lorentzian component.[17]

The other terms in Eq. (4.9) describe the damped fluctuations in the I_j, ϕ_3, and ϕ_+ variables and are of a much smaller magnitude than the leading term. These fluctuations decorrelate on typical time scales much smaller than that needed to see phase diffusion. Thus these fluctuations will show in the intensity spectrum as small but broad Lorentzian components. Previous calculations[13] have often been interested only in the spectral linewidth and have not studied these smaller fluctuation terms in detail. In the phase-sensitive measurements we describe later, these smaller terms become relevant and interesting, and are responsible for the nonclassical behavior.

Other correlation functions are similarly calculated. The results are symmetrical upon the interchange of $\hat{\Phi}_1$ and $\hat{\Phi}_2$, since $\kappa_1=\kappa_2$. It is straightforward to show that in the presence of phase diffusion the steady-state moments of the type $\langle \hat{\Phi}_1^\dagger(t)\hat{\Phi}_1^\dagger(t+\tau)\rangle$, $\langle \hat{\Phi}_2^\dagger(t)\hat{\Phi}_1(t+\tau)\rangle$, $\langle \hat{\Phi}_1(t)\rangle\cdots$ become zero.

We now wish to calculate stationary spectra. The results for the fluctuation spectrum are readily obtained from the following definition:

$$S_{ij}(\omega)=\int_{-\infty}^{\infty} e^{i\omega\tau}\langle \hat{\Phi}_i^\dagger(t)\hat{\Phi}_j(t+\tau)\rangle d\tau . \tag{4.10}$$

The cross-correlation spectrum $C_{ij}(\omega)$ is similarly defined as

$$\begin{aligned}C_{ij}(\omega)&=\int_{-\infty}^{\infty} e^{i\omega\tau}\langle \hat{\Phi}_i(t)\hat{\Phi}_j(t+\tau)\rangle d\tau , \\ C_{ij}^\dagger(\omega)&=\int_{-\infty}^{\infty} e^{i\omega\tau}\langle \hat{\Phi}_i^\dagger(t)\hat{\Phi}_j^\dagger(t+\tau)\rangle d\tau .\end{aligned} \tag{4.11}$$

When the integrals are performed the results are obtained in the form of Lorentzians. We find that $S_{12}(\omega)=S_{21}(\omega)=C_{11}(\omega)=C_{22}(\omega)=0$. The only nonzero cross-correlation spectra can be written in the form

$$\begin{aligned} S_{11}(\omega)=S_{22}(\omega)&=2I^0L_{\lambda_0}+\tfrac{1}{8}C_{I_-}(\omega)+\tfrac{1}{8}C_{\phi_+}(\omega)\\ &\quad+\tfrac{1}{8}C_{I_+}(\omega)\ ,\\ C_{12}(\omega)=C_{12}^{\dagger}(\omega)&=2I^0L_{\lambda_0}-\tfrac{1}{8}C_{I_-}(\omega)-\tfrac{1}{8}C_{\phi_+}(\omega)\\ &\quad+\tfrac{1}{8}C_{I_+}(\omega)\ , \end{aligned} \tag{4.12}$$

where

$$L_\lambda=2\lambda\kappa/(\lambda^2+\omega^2)\ ,$$

$$C_{I_-}(\omega)=-L_{(\lambda_0+2\kappa)}\ ,$$

$$C_{\phi_+}(\omega)=-\sum_{j=1}^{2}\kappa\left[\frac{\bar{A}_j^2}{2\bar{\lambda}_j}+\frac{\bar{A}_1\bar{A}_2}{\bar{\lambda}_1+\bar{\lambda}_2}\right]L_{(\bar{\lambda}_j+\lambda_0)}\ ,$$

$$C_{I_+}(\omega)=\sum_{j=1}^{2}\kappa\left[\frac{A_j^2}{2\lambda_j}+\frac{A_1A_2}{\lambda_1+\lambda_2}\right]L_{(\lambda_j+\lambda_0)}\ .$$

Here $\lambda_0=\kappa/8I_0$. We note that L_λ is obtained from

$$L_\lambda=\kappa\int_{-\infty}^{\infty}e^{i\omega\tau-\lambda|\tau|}d\tau\ . \tag{4.13}$$

The expressions L_{λ_0}, C_{I_-}, C_{ϕ_+}, and C_{I_+} are the different Lorentzian components corresponding to the different eigenvalues (0, 2κ, $\bar{\lambda}_{1,2}$, and $\lambda_{1,2}$) of the deterministic part of Eq. (3.7). These terms describe the diffusion of the phase-difference ϕ_- variable and the relaxation of the ΔI_-, $\Delta\phi_+$, and ΔI_+ variables, respectively.

The first term in the solutions for $S_{11}(\omega)$ and $C_{12}(\omega)$ is

$$2I^0L_{\lambda_0}=\frac{\frac{1}{2}}{(1/8I^0)^2+(\omega/\kappa)^2}\ . \tag{4.14}$$

This is the large but narrow spectral component due to the phase diffusion of the signal-idler phase-difference ϕ_-. The full width at half maximum (FWHM) of the Lorentzian is $2\kappa/8I^0$. Thus the width narrows with increasing pump power.

The second term in the solutions for $S_{11}(\omega)$ and $C_{12}(\omega)$ is derived from the intensity difference fluctuations $\langle\Delta I_-(t)\Delta I_-(t+\tau)\rangle$. For $1/8I^0\ll 2$, this becomes

$$C_{I_-}(\omega)=-L_{2\kappa}=-\frac{4}{4+(\omega/\kappa)^2}\ . \tag{4.15}$$

This is the spectral component due to fluctuations in the signal-idler intensity difference ΔI_-. This component was derived and discussed by Reynaud *et al.*[8] We notice a lower and broader Lorentzian compared to that describing the phase diffusion. The negative sign means fluctuations are reduced below the coherent shot-noise limit, the maximum reduction occurring at zero frequency $\omega=0$. The width of this broad component is 4κ, reflecting the time scale for relaxing of ΔI_- fluctuations, which is much shorter than that of phase diffusion. We notice that the fluctuations in the intensity difference are independent of the pump decay rate and pump intensity above threshold. The difference variables are decoupled from the pump equations, which remain coupled to the signal-idler system only through the signal-idler phase and intensity sum variables. The two components L_0 and $L_{2\kappa}$ are new in the nondegenerate spectrum, when compared to the degenerate spectrum discussed by Collett and Walls.[16]

The third component $C_{\phi_+}(\omega)$ in the spectrum $S_{11}(\omega)$ is due to fluctuations in the signal-idler phase sum ϕ_+. We define the scaled parameters

$$\bar{w}=\frac{w}{k},\quad r=\frac{\kappa_3}{\kappa},\quad P=\frac{|E|}{E_T}\ , \tag{4.16}$$

where E_T is the threshold value of the driving field amplitude. The phase sum fluctuations are decreased below the vacuum noise level, as were the intensity difference fluctuations. The spectral shape, however, is a much more complicated function of pump decay rate r and pump amplitude P, and can become two peaked as the phase-sum eigenvalues $\bar{\lambda}_{1,2}$ become complex. In this case we can write the spectrum as the sum of two Lorentzian components. We have for $\bar{\lambda}_1$ complex

$$\begin{aligned} C_{\phi_+}(\omega)=&\frac{\bar{B}(1/8I^0+\mathrm{Re}\bar{\lambda}_1/\kappa)+\bar{C}(\bar{\omega}+\mathrm{Im}\bar{\lambda}_1/\kappa)}{(1/8I^0+\mathrm{Re}\bar{\lambda}_1/\kappa)^2+(\bar{\omega}+\mathrm{Im}\bar{\lambda}_1/\kappa)^2}\\ &+\frac{\bar{B}(1/8I^0+\mathrm{Re}\bar{\lambda}_1/\kappa)-\bar{C}(\bar{\omega}-\mathrm{Im}\bar{\lambda}_1/\kappa)^2}{(1/8I^0+\mathrm{Re}\bar{\lambda}_1/\kappa)^2+(\bar{\omega}-\mathrm{Im}\bar{\lambda}_1/\kappa)^2}\ , \end{aligned} \tag{4.17}$$

where $\bar{\lambda}_1=\bar{\lambda}_2^{*}=\mathrm{Re}\bar{\lambda}_1+i\,\mathrm{Im}\bar{\lambda}_1$ and

$$\bar{B}=\frac{\left[\left[\mathrm{Re}\frac{\bar{\lambda}_1}{\kappa}\right](1-\mathrm{Im}\bar{A}^2)+2-r\right]}{|\bar{\lambda}/\kappa|^2}+\frac{(1+\mathrm{Im}\bar{A}^2)}{\mathrm{Re}\bar{\lambda}/\kappa}\ ,$$

$$\bar{C}=-\frac{\left[2\left[\mathrm{Re}\frac{\bar{\lambda}_1}{\kappa}\right]\mathrm{Im}\bar{A}-\left[\mathrm{Im}\frac{\bar{\lambda}_1}{\kappa}\right](1-\mathrm{Im}\bar{A}^2)\right]}{|\bar{\lambda}/\kappa|^2}\ ,$$

$$\mathrm{Im}\bar{A}=(\bar{A}_1-\bar{A}_1^{*})/2i=(2-r)/[8rP-(2-r)^2]^{1/2}\ .$$

For the case we consider here where $1/8I^0$ is very small ($1/8I^0\ll\mathrm{Re}\bar{\lambda}_1,\mathrm{Re}\bar{\lambda}_2$), we may simplify as follows:

$$C_{\phi_+}(\omega)=-\frac{4(r^2+\bar{\omega}^2)}{(2rP-\bar{\omega}^2)^2+\bar{\omega}^2(2+r)^2}\ . \tag{4.18}$$

Figure 1 plots this spectrum for various r and P. This spectrum has been derived and discussed in part by Reynaud *et al.*[8] and also Bjork and Yamamoto.[9] We point out that the limiting spectral fluctuations given by (4.15) and (4.18) are derivable by linearizing Eqs. (2.4) assuming a metastable phase and Fourier transforming to solve for the steady-state fluctuations.[8,9] Such an analysis, however, cannot predict the spectral component (4.14) which is caused by the diffusion in the signal-idler phase difference.

The fourth component $C_{I_+}(\omega)$ is the spectrum of fluc-

tuations in the signal-idler intensity sum I_+. For $1/8I^0$ very small ($I/8I^0 \ll \mathrm{Re}\lambda_1, \mathrm{Re}\lambda_2$), the result simplifies to

$$C_{I_+}(\omega)=\frac{4(r^2+\bar{\omega}^2)}{[2r(P-1)-\bar{\omega}^2]^2+\bar{\omega}^2 r^2} . \tag{4.19}$$

We notice an increase in the intensity sum fluctuations above the vacuum noise level. As with the phase sum spectrum $C_{\phi_+}(\omega)$, the shape $C_{I_+}(\omega)$ depends on the pump amplitude and decay rate (P and r). The spectrum may show a splitting into peaks where the eigenvalues $\lambda_{1,2}$ become complex.

At this point it is instructive to compare the solutions (4.12) for the nondegenerate parametric oscillator above threshold to those derived[16] for the degenerate parametric oscillator above threshold. For the latter one defines the pump mode $\hat{a}_3$ driven by the field E as before, and a cavity mode $\hat{a}_1$, both with corresponding c-number amplitudes defined in the positive P representation. One may transform to radial and phase variables and linearize about one of the stable steady states discussed in Refs. 15 and 16. We define $\alpha_1=\sqrt{I}e^{-i\phi}$ and derive the final result for the linearized fluctuations spectrum in agreement with the original expressions derived by Drummond *et al.*[15] and Collett and Walls,[16]

$$\begin{aligned} S_{11}(\omega)&=\tfrac{1}{8}C_\phi(\omega)+\tfrac{1}{8}C_I(\omega) , \\ C_{12}(\omega)&=-\tfrac{1}{8}C_\phi(\omega)+\tfrac{1}{8}C_I(\omega) . \end{aligned} \tag{4.20}$$

Here C_ϕ and C_I are directly related to the limiting solutions (4.18) and (4.19) for C_{ϕ_+} and C_{I_+} as follows: $C_\phi=2C_{\phi_+}$ and $C_I=2C_{I_+}$. The scaled parameters $\bar{\omega}$, r, and P have similar meanings in the degenerate case.

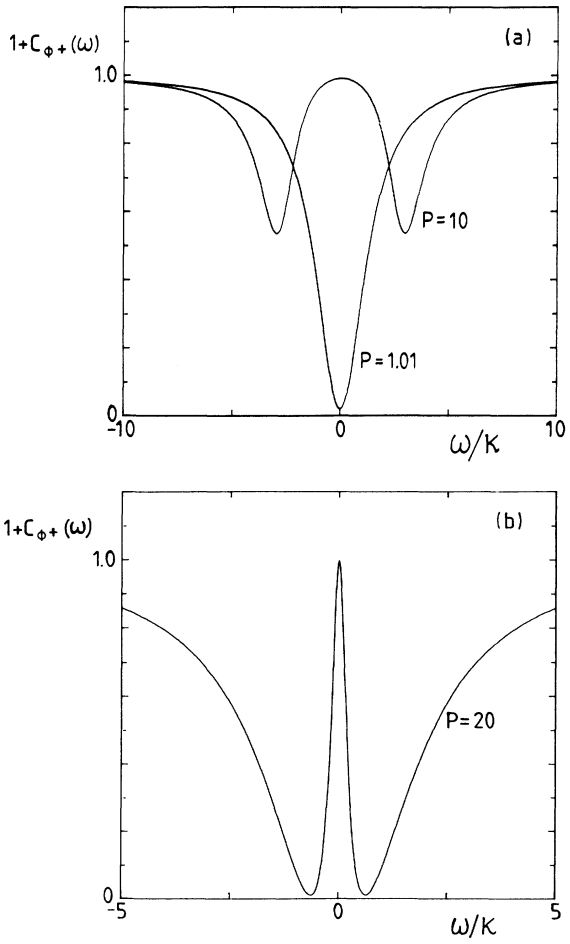

FIG. 1. Spectral fluctuations in the signal-idler phase sum: $1+C_{\phi_+}(\omega)$. (a) $r=0.1$, (b) $r=0.01$, $P=20$.

V. SQUEEZING MEASUREMENTS AND SPECTRA

We now discuss the various types of "squeezing" measurements and the corresponding squeezing spectra possible.

A. Intensity fluctuations

Perhaps the simplest type of measurement is direct detection of intensity fluctuations. In general, one can define intensity correlation spectra of the type

$$G_{ij}(\omega)=\int_{-\infty}^{\infty} e^{i\omega\tau}\langle \hat{I}_i(t),\hat{I}_j(t+\tau)\rangle d\tau , \tag{5.1}$$

where $\hat{I}_j=\hat{\Phi}_j^\dagger\hat{\Phi}_j$ is the external field operator and we use the notation $\langle x,y\rangle=\langle xy\rangle-\langle x\rangle\langle y\rangle$. The steady-state moments in the linearized approximation used here are rapidly expressed in terms of the stochastic variables, whose correlations correspond to time-ordered, normal-ordered[18] operator correlations.

We assume $[\hat{\Phi}_j(\tau),\hat{\Phi}_j^\dagger(0)]=\delta(\tau)$. We have

$$G_{ij}(\omega)=2\kappa I^0\delta_{ij}+4\kappa^2\int_{-\infty}^{\infty} e^{i\omega\tau}\langle \delta I_i(0)\delta I_j(\tau)\rangle d\tau . \tag{5.2}$$

The stochastic solutions δI_j have already been obtained [Eqs. (3.8) and (3.10)]. The intensity correlations depend only on the stable $\delta I_\pm$ subset and are independent of phase. Hence the solutions for the intensity correlation spectra are readily obtained by Fourier transforming the subset equations (3.7) and solving algebraically for $\delta I_-(\omega)$, $\delta I_+(\omega)$, and $\delta I_3(\omega)$ where, for example,

$$\delta I_-(\omega)=\frac{1}{\sqrt{2\pi}}\int_{-\infty}^{\infty} e^{i\omega t}\delta I_-(t)dt . \tag{5.3}$$

This is the approach used in a recent paper by Lane *et al.*[10]

A calculation of the reduction (or squeezing) in the intensity difference fluctuations was given by Reynaud *et al.*[8] Heidmann *et al.*[4] have measured the signal and idler intensity correlation above threshold and shown a reduction of intensity difference fluctuations below the shot-noise level. The signal and idler fields are spatially separated and impinge directly on two separate photodetectors. The fluctuations in the difference current from these detectors are then measured using a power spectrum analyzer. Thus one measures

$$S_D(\omega)=\int_{-\infty}^{\infty} e^{i\omega\tau}\langle \hat{I}_-(t),\hat{I}_-(t+\tau)\rangle d\tau , \tag{5.4}$$

where $\hat{I}_-=\hat{I}_1-\hat{I}_2=\hat{\Phi}_1^\dagger\hat{\Phi}_1-\hat{\Phi}_2^\dagger\hat{\Phi}_2$ is the external photon

difference operator. In terms of the stochastic quantities we have calculated, one rewrites[10]

$$S_D(\omega)=4\kappa I^0+4\kappa^2\int_{-\infty}^{\infty} e^{i\omega\tau}\langle \delta I_-(t)\delta I_-(t+\tau)\rangle d\tau \ . \tag{5.5}$$

The solution is obtainable directly from the intensity difference equations and solution (3.8). The result obtained by Lane *et al.*[10] is in agreement with that calculated by Reynaud *et al.*[8] The shot-noise level is the noise level corresponding to uncorrelated coherent fields at the signal and idler detectors. This corresponds to the normally ordered variances and covariances given by the stochastic variables in the P representation becoming zero. Thus the shot-noise level is $4\kappa I^0$, and hence one can define the normalized intensity difference squeezing spectrum

$$\bar{S}_D(\omega)=\frac{S_D(\omega)}{4\kappa I^0}=1-L_{2\kappa} \ . \tag{5.6}$$

B. Single local oscillator experiments

We now discuss phase-sensitive measurements performed with the use of a strong external local oscillator, phase shifted in some manner with respect to the pump field whose reference phase we take to be zero. There are two types of local oscillator measurements one can perform. The first type is the traditional squeezing measurements with nondegenerate signal and idler frequencies, where a single local oscillator beats with the combined signal and idler fields, on the surface of a single photodetector. The resulting photocurrent fluctuations are analyzed with a power spectrum analyzer. This experiment has been performed by Slusher *et al.*[24] for a nondegenerate four-wave mixer below threshold. The measurable output of the spectrum analyzer is directly related to fluctuations in a combined signal and idler quadrature operator. This type of squeezing was first discussed by Caves and Schumaker[25] and Yurke[26] and others.[12,27] In particular, we use here the results and notation of Drummond and Reid[18] in the limit of perfect efficiency. We define this squeezing spectrum to be

$$V(\theta,\omega)=1+\int_{-\infty}^{\infty} e^{i\omega\tau}\langle :\hat{X}_\theta(0)\hat{X}_\theta(\tau):\rangle d\tau \ , \tag{5.7}$$

where

$$\hat{X}_\theta(t)=\sum_{j=1}^{2} e^{i\theta+i\omega_0 t}\hat{\Phi}_j(t)+\text{H.a.} \tag{5.8}$$

Here θ is the phase angle between the local oscillator and the pump field, which we have taken to be real for convenience. The frequency $\omega_0=\omega_3/2$ is the local oscillator frequency, and H.a. is the hermitian adjoint. In terms of the stochastic variables $S_{ij}(\omega)$ and $C_{ij}(\omega)$ of Eqs. (4.10) and (4.11), the squeezing spectrum becomes[18,12]

$$V(\theta,\omega)=1+S^{(1)}(\theta,\omega-\epsilon)+S^{(1)}(\theta,-\omega-\epsilon) \ , \tag{5.9}$$

where

$$S^{(1)}(\theta,\omega)=S_{11}(\omega)+S_{22}(-\omega)+2\,\mathrm{Re}[e^{2i\theta}C_{21}(\omega)] \ .$$

The total spectrum $V(\theta,\omega)$ is symmetric about $\omega=0$ (corresponding to the local oscillator frequency ω_0). It comprises two mirror image components centered at frequencies $\omega=\pm\epsilon$ (corresponding to the cavity resonant frequencies $\omega_{1,2}$). These mirror spectra are nonoverlapping and can attain a minimum value of $S^{(1)}(\theta,\omega)=-1$. We have squeezing when $V(\theta,\omega)<1$, so that the noise is reduced below the shot- (or coherent-) noise level. It is sufficient to examine the behavior of the function $S^{(1)}(\theta,\omega)$ and realize one has squeezing when $S^{(1)}(\theta,\omega)<0$. Perfect squeezing corresponds to $S^{(1)}(\theta,\omega)=-1$. The squeezing in the vicinity of $\omega=\epsilon$ may be written approximately as

$$V(\theta,\nu+\epsilon)=1+S^{(1)}(\theta,\nu) \ , \tag{5.10}$$

where we have defined ν as the displacement from the frequency ϵ ($\omega=\nu+\epsilon$).

The phase θ of the local oscillator may be varied to change the particular quadrature detected. To minimize the noise (optimize squeezing) we choose $\theta=\pi/2$. The squeezing in the vicinity of $\omega=\epsilon$ becomes

$$V\left[\frac{\pi}{2},\nu+\epsilon\right]=1-\tfrac{1}{2}[C_{I_-}(\nu)+C_{\phi_+}(\nu)] \ . \tag{5.11}$$

We notice the dual cancellation, for this choice of $\theta=\pi/2$, of the phase difference and intensity sum fluctuations, which show noise increased above the coherent-noise level. In particular, the very large noise contribution due to the phase diffusion is absent. For this optimal angle, the fluctuations may be reduced significantly below the vacuum level. Thus squeezing of fluctuations is possible in a particular combination of signal-idler quadrature amplitudes because the quantum noise of each is correlated. This correlation is seen most readily in dual local oscillator experiments and is explained further in Sec. V C.

We discuss now the shape of this optimal noise spectrum. The minimum noise is sensitive only to the small quantum fluctuations in the signal-idler sum phase and intensity difference. The spectrum of fluctuations $-L_{2\kappa}$ in the intensity difference is the simple inverted Lorentzian described by Eq. (4.15). The shape is independent of pump relaxation and power (r and P).[8] This intensity fluctuation (or correlation) spectrum is directly observable in the Heidmann *et al.*[4] measurement of the intensity-difference fluctuation spectrum. However, because the external local oscillator quadrature phase measurement is sensitive to *both* phase and intensity fluctuations, we need here a reduction of noise in both quantities to obtain total noise suppression. The shape of the phase fluctuation spectrum is sensitive to pump decay rate and power. For this reason, we shall treat the different regimes of decay rates separately.

In the limit of a very bad pump, $r\to\infty$ ($\kappa_3\gg\kappa$), the spectrum is particularly easy to solve. One may either take the limit of the general solutions or else derive from first principles by adiabatically eliminating the pump variables. The minimum noise spectrum is (noting that in the limit we consider here, $1/8I^0\ll 1$)

$$V\left[\frac{\pi}{2},\nu+\epsilon\right]=1-\frac{2}{4+(\nu/\kappa)^2}-\frac{2}{4P^2+(\nu/\kappa)^2}\ . \tag{5.12}$$

This expression includes both the intensity-difference and phase-sum fluctuations.

This spectrum in the "bad-pump" limit is plotted in Fig. 2. Near threshold, $P=1$, the phase and intensity fluctuations are both simple inverted Lorentzians with width (FWHM) 4κ and minimum noise at $\omega=0$. We have near perfect noise reduction at $\omega=0$. On increasing the pump power P, the intensity fluctuations are unchanged, but the phase fluctuations increase, reaching the vacuum noise level for large P. At higher pump powers, the reduction in noise (50% of the vacuum noise level at zero frequency) is due solely to signal-idler intensity correlations. This reduction in noise is not seen in degenerate parametric oscillation.[16] A linearized calculation of optimal noise in the degenerate case reveals

$$V\left[\frac{\pi}{2},\nu+\epsilon\right]=1-C_\phi(\nu)=1-\frac{4}{4P^2+(\nu/\kappa)^2}\ . \tag{5.13}$$

This is a measure of the signal phase fluctuations alone, since the intensity correlations do not contribute to the squeezing in the degenerate case. Clearly there is no squeezing in the degenerate case as $P\to\infty$, although there is in the nondegenerate case.

Figures 3 and 4 plot the noise spectrum for cavities where the pump and signal and idler cavity decay rates are of the same order. The zero frequency part of the spectrum is independent of the ratio of decay rates. Also as emphasized above, the intensity fluctuations do not depend on r and P. The phase fluctuations do show a different spectral structure. With sufficient pump intensity P, the phase spectrum shows two sidedips. This is distinct from the intensity fluctuation spectrum which causes a center dip. The splitting of the phase fluctuation spectrum is expected in view of the eigenvalue solutions (4.17). The phase eigenvalues $\bar{\lambda}_{1,2}$ become complex and we expect oscillatory behavior in the two-time correlation

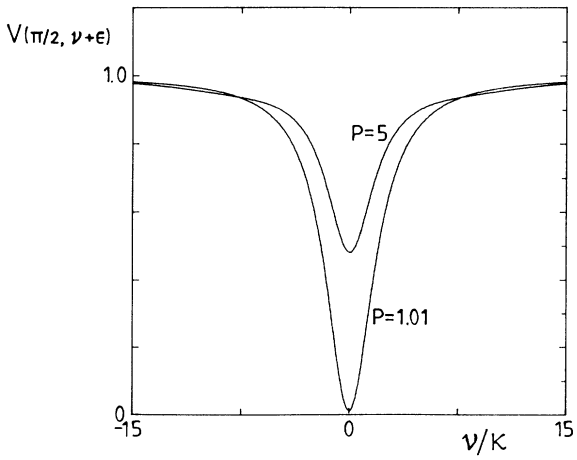

FIG. 2. Spectral squeezing in the signal-idler combined quadrature: Plot of $V(\pi/2,\nu+\epsilon)$. "Bad" pump limit $r=10$. Various pump intensities.

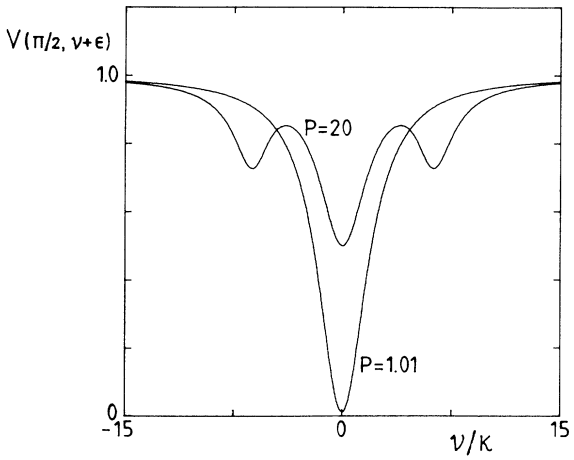

FIG. 3. Spectral squeezing $V(\pi/2,\nu+\epsilon)$, $r=1$. Various pump intensities.

functions. A comparison with solution (4.18) shows that larger reductions in phase fluctuations occur with decreasing r (as κ_3 decreases relative to κ). For $r=0.1$, we have perfect intensity correlation at zero frequency, and near perfect phase correlation at the outer frequency ($\omega\sim 3$ for $P=50$).

Figure 5 shows the optimal fluctuation spectrum in the limit of a very good pump ($r\to 0$). The phase fluctuation spectrum in this limit has two minima, at $\nu/\kappa\sim\pm\sqrt{2rP}$. The minima show that perfect reduction in phase fluctuations occurs at frequencies $\nu/\kappa\sim\sqrt{2rP}$. The intensity fluctuations are near perfectly reduced at these low frequencies ($\nu<\kappa$). Hence we may obtain total suppression of noise in $V(\pi/2,\nu+\epsilon)$ for a large range of pump powers P.

The minimum noise quantity $V(\pi/2,\nu+\epsilon)$, Eq. (5.11), is in a combined quadrature which has neither very large phase fluctuations nor large intensity fluctuations $C_{I_+}(\omega)$. Upon varying the phase angle θ, however, the noise increases as these large fluctuations are detected. The fluctuations in phase are so large that even small changes in phase angle θ, as might be expected in an ex-

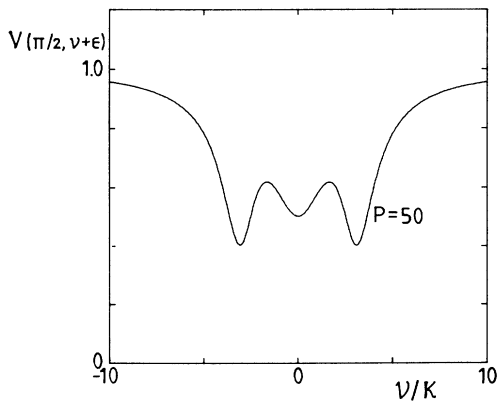

FIG. 4. Spectral squeezing $V(\pi/2,\nu+\epsilon)$, $r=0.1$, $P=50$.

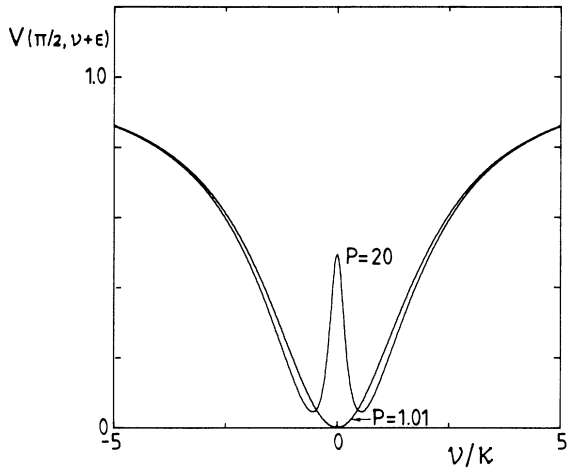

FIG. 5. Spectral squeezing $V(\pi/2,\nu+\epsilon)$, $r=0.01$. Various pump intensities.

perimental situation, will allow detection of the narrow phase diffusion spectral component. This shows up as an increase in noise over the bandwidth of the Lorentzian L_{λ_0} [Eq. (4.14)]. For θ not quite optimal, the noise spectrum can therefore be written

$$V(\theta,\nu+\epsilon)=1+2[S_{11}(\nu)-jC_{12}(\nu)] , \tag{5.14}$$

where $j=\langle\cos 2\Delta\theta\rangle$ is the average over the phase jitter $\Delta\theta$. Figure 6 illustrates the appearance of the phase noise. The effect of phase diffusion, in practice, is to eliminate the squeezing at zero frequency.

C. Dual-local oscillator experiments

A second type of external local oscillator experiment involves separating the signal and idler beams spatially and combining each with its own local oscillator, using two photodetectors. One then adds or subtracts the individual photocurrents and measures the power spectrum or current fluctuations in this combined current. This scheme corresponds to that obtained with orthogonal polarizations incident on a single photodetector. Each polarization is detected individually in this case and the output is the sum of the two currents. This general type of measurement has been discussed previously by Schumaker *et al.*[28,29] and Levenson and Shelby.[29] The output power spectrum is a measure of the spectrum of fluctuations in the signal-idler quadrature phase amplitude sum or difference. Thus we define[18]

$$\Delta^2(\theta_1,\theta_2,g,\omega) = \int_{-\infty}^{\infty} e^{i\omega\tau}\langle[\hat{X}_1^{\theta_1}(0)-g\hat{X}_2^{\theta_2}(0)] \times[\hat{X}_1^{\theta_1}(\tau)-g\hat{X}_2^{\theta_2}(\tau)]\rangle d\tau . \tag{5.15}$$

Since the currents may be individually amplified, we introduce the relative amplification factor g.[29] Although this equation is for current differences, it also describes current sums when $g<0$. The solution for the spectrum becomes[18]

$$\Delta^2(\theta_1,\theta_2,g,\omega)=1+g^2+2\,\mathrm{Re}\{S_{11}(\omega)+g^2S_{22}(\omega)-ge^{i(\theta_1+\theta_2)}[C_{12}(\omega)+C_{21}(\omega)]\} . \tag{5.16}$$

A reduction of fluctuations in this quadrature amplitude difference is indicative of a correlation between the amplitudes in frequency space. We define normalized quadratures as (T is the detection time)

$$\hat{x}_j^{\theta_j}(\omega)=\frac{1}{\sqrt{T}}\int_{-T/2}^{T/2} e^{i\omega t}\hat{X}_j^{\theta_j}(t)dt \tag{5.17}$$

and consider the Hermitian real and imaginary parts of these operators. It is possible to show[18] that

$$\Delta^2(\theta_1,\theta_2,g,\omega)=\langle\hat{x}_-(\omega)^\dagger\hat{x}_-(\omega)\rangle , \tag{5.18}$$

where $\hat{x}_-(\omega)=\hat{x}_1^{\theta_1}(\omega)-g\hat{x}_2^{\theta_2}(\omega)$. Thus $\Delta^2(\theta_1,\theta_2,g,\omega)$ is the average difference between $\hat{x}_1^{\theta_1}(\omega)$ and $g\hat{x}_2^{\theta_2}(\omega)$. It may be thought of as the average error in inferring the signal amplitude $\hat{x}_1^{\theta_1}(\omega)$ as $g\tilde{x}_2^{\theta_2}(\omega)$, where $\tilde{x}_2^{\theta_2}(\omega)$ is the result of measurement of $\hat{x}_2^{\theta_2}(\omega)$. We note that the vacuum-noise level of the signal amplitude $\hat{x}_1^{\theta_1}(\omega)$ alone is 1. Hence where $\Delta^2(\theta_1,\theta_2,g,\omega)<1$, the average error in

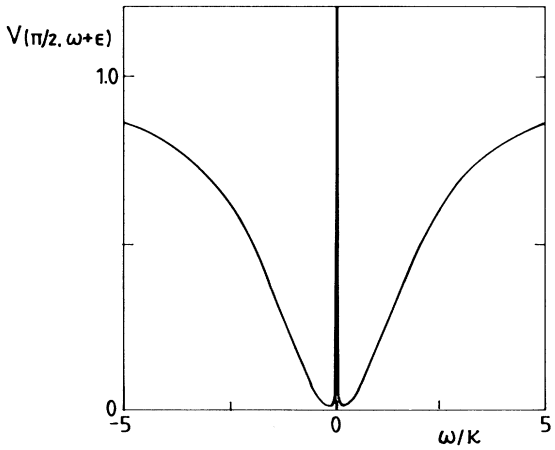

FIG. 6. Effect of phase diffusion in external local oscillator measurements where the effect of phase jitter is to produce noise near $\omega=0$. Here $P=1.01$, $r=0.01$.

our estimate of the signal by measurement of the idler is below the vacuum-noise level of the signal. The quantity $\Delta^2(\theta_1,\theta_2,g,\omega)$ is thus closely related to ideas of quantum-nondemolition (QND) measurement and state reduction.[30]

If we consider the combined quadrature

$$\hat{x}_-(\omega)=\hat{x}_1^{\theta_1}(\omega)-g\hat{x}_2^{\theta_2}(\omega)\ , \tag{5.19}$$

a squeezing occurs when the noise falls below the total vacuum-noise level, i.e., $\Delta^2(\theta_1,\theta_2,g,\omega)<1+g^2$. This is also equivalent to violating a "normally ordered" Cauchy-Schwarz inequality

$$\langle :\hat{x}_1^{\theta_1}(\omega)^\dagger\hat{x}_1^{\theta_1}(\omega):\rangle\langle :\hat{x}_2^{\theta_2}(\omega)^\dagger\hat{x}_2^{\theta_2}(\omega):\rangle \geq|\langle\hat{x}_1^{\theta_1}(\omega)^\dagger\hat{x}_2^{\theta_2}(\omega)\rangle|^2\ , \tag{5.20}$$

which is satisfied by classical radiation fields.[18] Such a squeezing brought about by nonclassical correlations has been demonstrated by Schumaker *et al.*, and Levenson and Shelby.[29]

The $\Delta^2(\theta_1,\theta_2,g,\omega)$ has a different shape depending on the value of g chosen. First we wish to choose g to minimize the squeezing spectrum. The squeezing spectrum is always normalized to the total vacuum-noise level. Thus the squeezing spectrum is defined,

$$V(\theta_1,\theta_2,g,\omega)=\Delta^2(\theta_1,\theta_2,g,\omega)/(1+g^2)\ , \tag{5.21}$$

where $\Delta^2(\theta_1,\theta_2,g,\omega)$ is given by (5.15) and (5.18). A check shows that for this symmetrical situation where $\langle(\hat{X}_1^{\theta_1})^2\rangle=\langle(\hat{X}_2^{\theta_2})^2\rangle$, $V(\theta_1,\theta_2,g,\omega)$ is minimized for $g^2=1$. Thus (we take $g=1$)

$$V(\theta_1,\theta_2,\omega)=1+S_{11}(\omega)+S_{22}(\omega) -\mathrm{Re}\{e^{i(\theta_1+\theta_2)}[C_{12}(\omega)+C_{21}(\omega)]\}\ . \tag{5.22}$$

Because for our particular example we have $S_{11}(\omega)=S_{22}(\omega)=S_{11}(-\omega)=S_{22}(-\omega)$ and $C_{12}(\omega)=C_{21}(\omega)$, this double-local-oscillator spectrum has a similar shape to the squeezing spectrum [(5.9), (5.10)] for a single local oscillator. The squeezing spectrum is minimized for $\theta_1=-\theta_2$ for the case of $g=1$. (We note that in the case of current summing with orthogonal polarizations the phase angles will depend on the local-oscillator polarization. For plane polarization, typically $\theta_1=\theta_2$.) The optical squeezing is then

$$V(\theta_1-\theta_1,\omega)=1-\tfrac{1}{2}[C_{I_-}(\omega)+C_{\phi_+}(\omega)]\ . \tag{5.23}$$

This spectral shape is identical to the one discussed above and depicted in Figs. (2)–(5). A maximum reduction in shot noise is possible. This corresponds to a maximum correlation of quadrature phase amplitudes according to quantum mechanics.[18]

With the choice of quadrature angles $\theta_2=-\theta_1$ we see that the noise in the signal-idler amplitude difference $(\hat{X}_1^{\theta_1}-\hat{X}_2^{-\theta_1})$ is independent of the larger fluctuations in the signal-idler intensity and phase. This significant reduction of fluctuations is brought about by the correlation between the signal and idler phase and intensities. Figure 7 gives a schematic diagram of the correlation. The coherent amplitude of the signal and idler is depicted by the upper and lower diagrams, respectively. The intensity is a stable quantity and hence is depicted undergoing only small rapid (quantum) fluctuations about the circumference. Because the signal and idler fields have correlated intensity, the fluctuations in the intensity difference are hence much smaller than the intensity fluctuations themselves. The individual signal and idler phasors undergo phase diffusion. The phase fluctuation is significant over larger time intervals. Again, however, the drift in phase of signal and idler is correlated in such a way that the fluctuations in the sum phase $(\theta_1+\theta_2)$ are very small (unnoticeable in the diagram). It is clear from Fig. 7 that the projections $\hat{X}_1^0-X_2^0$ and $\hat{X}_1^{\pi/2}-\hat{X}_2^{-\pi/2}$ will not show the larger fluctuations in the signal and idler phase and intensity. The fluctuations in these combinations of quadrature phases are very much reduced and sensitive only to the much smaller fluctuations in the signal-idler intensity-difference or phase-sum variables.

We may also understand from this picture the reason for substantial squeezing in the single local oscillator experiment for the choice of phase angle $\theta=\pi/2$. From Eq. (5.8) we see that this corresponds to measuring experimentally the fluctuations in the combined quadrature amplitude $\hat{X}_1^{\pi/2}+\hat{X}_2^{\pi/2}$. Figure (7) shows that this is a quiet quantity insensitive to the larger phase and intensity fluctuations. Similar behavior will clearly occur in single local oscillator experiments with orthogonal polarizations, as evidenced by Eq. (5.23).

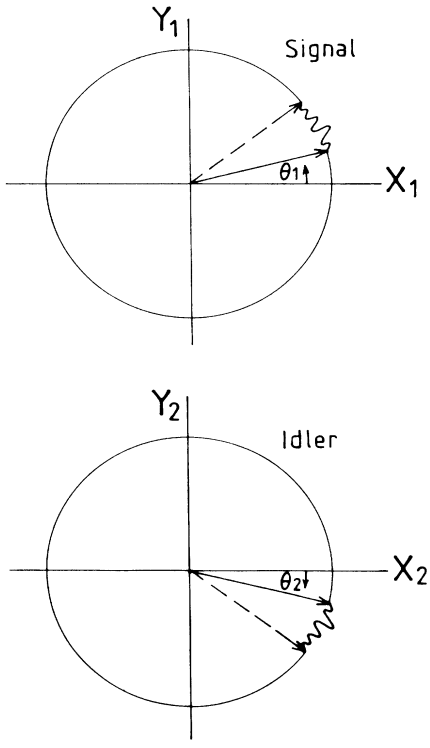

FIG. 7. Correlation of signal and idler quadrature phase amplitudes: We use the notation $X_i=X_i^0$ and $Y_j=X_j^{\pi/2}$.

D. Quadrature phase inference experiments

Of particular interest is the case where g is chosen to minimize the error quantity $\Delta^2(\theta_1,\theta_2,g,\omega)$ itself.[29] Given a result $\tilde{x}^{\theta_2}_2(\omega)$ for the idler measurement, we can estimate the signal $\hat{X}^{\theta_1}_1(\omega)$ as $\tilde{g}\tilde{x}^{\theta_2}_2(\omega)$. The choice of $g=\tilde{g}$ is defined as that required to minimize the average error associated with this inference. By differentiation[18] we have

$$\tilde{g}=\frac{C_{12}(\omega)+C_{21}(\omega)}{1+2S_{22}(\omega)} . \tag{5.24}$$

With this value of $\tilde{g}$, the minimum variance $\Delta^2(\theta_1,\theta_2,g,\omega)$ becomes [we have simplified for our example where $S_{11}(\omega)=S_{22}(\omega)$ and $C_{12}(\omega)=C_{21}(\omega)$]

$$\Delta^2(\theta_1,\omega)=\frac{[1+2S_{11}(\omega)]^2-4C_{12}(\omega)^2}{1+2S_{11}(\omega)} . \tag{5.25}$$

Note that we have also chosen $\theta_2=-\theta_1$ to minimize $\Delta^2(\theta_1,\theta_2,g,\omega)$ with respect to the choice of phase angle θ_2. Figure 8 plots this quantity $\Delta^2(\theta_1,\omega)$ for various parameters. When $\Delta^2(\theta_1,\omega)<1$, this can violate an inferred Heisenberg uncertainty principle.[18,31] This is an example of macroscopic EPR correlations, since the photon number can be large.

E. Phase fluctuations

The measurements discussed above involve external local oscillators. By this we mean a strong field which is phase locked to that of the pump field. Because there is no phase locking of the individual signal or idler fields to this pump phase, this local oscillator measurement which measures fluctuations along a projection will always see fluctuations in both signal intensity and phase (Fig. 7). Intensity fluctuations alone are measurable with direct detection. A direct measurement of phase fluctuations alone is more difficult. Ideally one would like to adjust the local oscillator phases θ_1 and θ_2 to keep track of the diffusing signal-idler phases and select to measure fluctuations in the quadrature at $\pi/2$ to this phase. This becomes feasible far enough above threshold where the phase diffusion slows down.

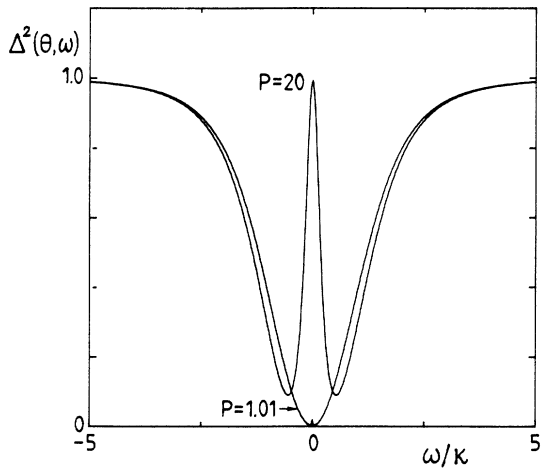

FIG. 8. Inference spectrum $\Delta^2(\theta_1,\omega)$, $r=0.01$.

An example is the phase-shifting interferometer developed by Levenson *et al.*[32] The phase-shifting interferometer is resonant with the large-intensity "coherent" peak, but nonresonant with the sideband frequencies. Thus one can make use of the different coherence times, or different bandwidths, of the phase-diffusing component and the smaller incoherent components. The interferometer resonant with the large coherent component has the effect of phase shifting this component with respect to the sidebands. The light reflected off the interferometer is composed of the (unchanged) sidebands, and over narrower frequencies, the coherent part with a phase shift. If this reflected field then impinges on a photodetector, the phase-shifted coherent part of the field acts like a local oscillator for the sidebands.

With careful selection of the phase shift θ, one can measure a particular quadrature phase relative to the original phase of the coherent (phase-diffusing) amplitude. This phase shifting of the coherent amplitude relative to the sidebands will work only if the amplitude has stable phase over the storage time of the field in the interferometer. Thus a long coherence time is required for the phase diffusion. If this is possible, one can then adjust θ to measure directly the phase fluctuations of the signal (or idler) field by choosing $\theta=\pi/2$.

Suppose two local oscillators (or phase shifters) and detectors are used for each of the signal and idler fields. If the resulting photocurrents are added, one might measure directly the phase sum of the signal-idler fields. The solution (4.18) and Fig. 1 shows a large squeezing possible in the phase sum fluctuations in two regimes. The first, discussed by Bjork and Yamamoto[9] is at lower frequencies near the threshold for oscillation ($P\sim 1$). The second regime occurs at all pump intensities but corresponds to excellent pump ($r\sim 10$), and is at higher frequencies. A similar limit exists for phase fluctuations in the degenerate case and has been discussed by Collett and Walls[16] and Savage and Walls.[34] An experiment of a similar type has been performed by Shelby *et al.*[32] and Schumaker *et al.*[29] who phase shifted a very stable but nontheless steadily phase-diffusing pump field relative to squeezed sideband vacuum components.

This direct rotating quadrature-phase measurement assumes essentially a stable phase for the coherent part of the field. It is the limit that has been of interest in the works of Reynaud *et al.*[8] and Björk and Yamamoto,[9] who calculate phase and intensity fluctuations by linearizing about a coherent signal or idler amplitude. The validity of this approximation depends on the time scale of the phase instability. A similar problem was analyzed recently by Drummond and Reid,[34] who showed that very long time-scales are indeed necessary.

VI. CONCLUSION

We have presented an analysis of the nondegenerate parametric oscillator above threshold. Unlike previous analyses we calculate the effect of the internal phase

diffusion on the different types of external squeezing measurements. The solutions are valid in the limit of large threshold photon number ($\kappa_3\kappa/g^2$) where one can linearize the effect of stable fluctuations. The experiments measuring intensity fluctuations are insensitive to phase as discussed by Reynaud *et al.*[8] and Lane *et al.*[10] and show no extra noise due to phase diffusion.

We are chiefly interested in squeezing experiments which use external local oscillators phase shifted with respect to the pump phase. The treatment shows that a correlation between signal and idler phase diffusion exists. Hence that the sum-phase fluctuations are not affected by this noise, and in fact are squeezed. Thus one can detect a particular combination of quadrature amplitudes and obtain in principle a squeezing of quantum fluctuations at all frequencies. This can occur even in the presence of quite significant phase diffusion.

However, because of the large size of the phase fluctuations and because a realistic external local oscillator will have some phase drift, the result for an experimental situation is a destroying of squeezing at low frequencies. We have calculated the bandwidth of this effect and discussed the squeezing possible at higher frequencies for certain optimal angles and certain cavity parameters.

We have analyzed squeezing measurements which use either one or two local oscillators. The twin local oscillator measurements can be used for nonlocal inference measurements of the EPR type. In these measurements, one quadrature measurement is used to infer the quadrature result at the other detector. A violation of an inferred Heisenberg uncertainty principle is possible. Finally, we mention that since the phase diffusion rate decreases sufficiently far above threshold it seems possible to make quadrature phase measurements relative to the signal or idler amplitude itself.

Note added in proof

Recent computer simulations[35] of the positive P representation for a nonlinear absorber have shown that quasiprobability distribution equations can become inequivalent to master equations at very large nonlinear damping. This limit is for $\kappa_3\kappa/g^2 \leq 1$ in our notation. The quasiprobability equations are derived using partial integration with the assumption of vanishing boundary terms. It seems that the boundary terms can be nonvanishing in the limit of large nonlinear absorption. In fact, the vanishing of boundary terms is a generic requirement with all stochastic techniques, and it remains to be verified that these vanish in our case. However, our master equation differs substantially from that for the nonlinear absorber, and computer simulations indicate that correct results are obtainable even in the limit of large nonlinearity.

Of course, this region is a different physical domain to the one of present interest, in which we treat the experimentally accessible limit of relatively large photon numbers and low quantum noise, with $\kappa_3\kappa/g^2 \gg 1$.

ACKNOWLEDGMENTS

This research has been supported by the New Zealand Universities Grants Committee.

[1]J. Opt. Soc. Am. B **4**, (1987), special issue "Squeezed States of the Electromagnetic Field", edited by H. J. Kimble and D. F. Walls; J. Mod. Opt. **34**, (1987), special issue edited by R. Loudon and P. Knight.

[2]M. Xiao, L. Wu, and H. J. Kimble, Phys. Rev. Lett. **59**, 278 (1987).

[3]C. M. Caves, Phys. Rev. D **26**, 1817 (1980).

[4]A. Heidmann, R. J. Horowicz, S. Reynaud, E. Giacobino, C. Fabre, and G. Cany, Phys. Rev. Lett. **59**, 2555 (1987).

[5]S. Machida, Y. Yamamoto, and J. Itaya, Phys. Rev. Lett. **58**, 1060 (1987).

[6]D. C. Burnham and D. L. Weinberg, Phys. Rev. Lett. **25**, 84 (1970); S. Friberg, C. K. Hong, and L. Mandel, *ibid.* **54**, 2011 (1985); E. Jakeman and J. G. Walker, Opt. Commun. **55**, 219 (1985); C. K. Hong and L. Mandel, Phys. Rev. Lett. **56**, 58 (1986); R. Brown, E. Jakeman, E. Pike, J. Rarity, and P. Tapster, Europhys. Lett. **2**, 279 (1986).

[7]Z. Y. Ou and L. Mandel, Phys. Rev. Lett. **61**, 50 (1988); **61**, 54 (1988).

[8]S. Reynaud, C. Fabre, and E. Giacobino, J. Opt. Soc. Am. B **4**, 1520 (1987).

[9]G. Bjork and Y. Yamamoto, Phys. Rev. A **37**, 125; **37**, 1991 (1988).

[10]A. S. Lane, M. D. Reid, and D. F. Walls, Phys. Rev. A **38**, 788 (1988).

[11]M. D. Reid and P. D. Drummond, Phys. Rev. Lett. **60**, 2731 (1988).

[12]M. J. Collett and R. Loudon, J. Opt. Soc. Am. B **4**, 1520 (1987).

[13]R. Graham and H. Haken, Z. Phys. **210**, 319 (1968); **211**, 469 (1968); R. Graham, Phys. Lett. **32A**, 373 (1970).

[14]K. J. McNeil and C. W. Gardiner, Phys. Rev. A **28**, 1560 (1983).

[15]P. D. Drummond, K. J. McNeil, and D. F. Walls, Opt. Acta **27**, 321 (1980); **28**, 211 (1981).

[16]M. J. Collett and D. F. Walls, Phys. Rev. A **32**, 2887 (1985).

[17]W. Brunner and H. Paul, in *Progress in Optics XV*, edited by E. Wolf (North-Holland, Amsterdam, 1977).

[18]P. D. Drummond and M. D. Reid (unpublished).

[19]P. D. Drummond, and C. W. Gardiner, J. Phys. A **13**, 2353 (1980).

[20]M. Wolinsky and H. Carmichael, Phys. Rev. Lett. **60**, 1836 (1988).

[21]W. H. Louisell, *Quantum Statistical Properties of Radiation* (Wiley, New York, 1973).

[22]L. Mandel, Phys. Rev. **144**, 1071 (1966), R. J. Cook, Phys. Rev. A **25**, 2164 (1982).

[23]M. J. Collett and C. W. Gardiner, Phys. Rev. A **30**, 1386 (1984); C. W. Gardiner and M. J. Collett, *ibid.* **31**, 3761 (1985).

[24]R. E. Slusher, L. W. Hollberg, B. Yurke, J. S. Mertz, and J. F. Valley, Phys. Rev. Lett. **55**, 2409 (1985).

[25]C. M. Caves and B. L. Schumaker, Phys. Rev. A **31**, 3068 (1985); B. L. Schumaker and C. M. Caves, *ibid.* **31**, 3093

(1985).
[26]B. Yurke, Phys. Rev. A **32**, 300 (1985).
[27]M. D. Reid and D. F. Walls, Phys. Rev. A **34**, 4929 (1986).
[28]B. L. Schumaker, J. Opt. Soc. Am. A **2**, 92 (1985).
[29]B. L. Schumaker, S. H. Perlmuter, R. M. Shelby, and M. D. Levenson, Phys. Rev. Lett. **58**, 357 (1987); M. D. Levenson and R. M. Shelby, J. Mod. Opt. **34**, 755 (1987).
[30]C. M. Caves, K. S. Thorpe, R. Drever, V. D. Sandberg, and M. Zimmerman, Rev. Mod. Phys. **52**, 341 (1980).
[31]M. D. Reid, Phys. Rev. A **40**, 913 (1989).
[32]M. D. Levenson, R. M. Shelby, M. D. Reid, D. F. Walls, and A. Aspect, Phys. Rev. A **32**, 1550 (1985); R. M. Shelby, M. D. Levenson, S. H. Perlmutter, R. S. Devoe, and D. F. Walls, Phys. Rev. Lett. **57**, 691 (1986).
[33]C. M. Savage and D. F. Walls, J. Opt. Soc. Am. B **4**, 1514 (1987).
[34]P. D. Drummond and M. D. Reid, Phys. Rev. A **37**, 1806 (1988).
[35]A. Smith and C. W. Gardiner, Phys. Rev. A **39**, 3511 (1989); I. J. D. Craig and K. J. McNeil, *ibid.* **39**, 6267 (1989).